Relationship between baseline brain metabolism measured using [18F]FDG PET and memory and executive function in prodromal and early Alzheimer's disease

**Christian Habeck · Shannon Risacher · Grace J. Lee ·
M. Maria Glymour · Elizabeth Mormino ·
Shubhabrata Mukherjee · Sungeun Kim ·
Kwangsik Nho · Charles DeCarli · Andrew J. Saykin ·
Paul K. Crane · for the Alzheimer's Disease
Neuroimaging Initiative**

Abstract Differences in brain metabolism as measured by
FDG-PET in prodromal and early Alzheimer's disease (AD)
have been consistently observed, with a characteristic pari-
etotemporal hypometabolic pattern. However, exploration
of brain metabolic correlates of more nuanced measures of
cognitive function has been rare, particularly in larger sam-
ples. We analyzed the relationship between resting brain
metabolism and memory and executive functioning within
diagnostic group on a voxel-wise basis in 86 people with
AD, 185 people with mild cognitive impairment (MCI), and
86 healthy controls (HC) from the Alzheimer's Disease
Neuroimaging Initiative (ADNI). We found positive associ-
ations within AD and MCI but not in HC. For MCI and AD,
impaired executive functioning was associated with reduced
parietotemporal metabolism, suggesting a pattern consistent
with known AD-related hypometabolism. These associa-
tions suggest that decreased metabolic activity in the parietal
and temporal lobes may underlie the executive function

C. Habeck (✉)
Cognitive Neuroscience Division, The Taub Institute for Research
on Aging and Alzheimer's Disease, Columbia University,
New York, NY, USA
e-mail: ch629@columbia.edu

S. Risacher · S. Kim · K. Nho · A. J. Saykin
Department of Radiology and Imaging Sciences, Center for
Neuroimaging, Indiana University School of Medicine,
Indianapolis, IN, USA

G. J. Lee
Department of Neurology, University of California at Los Angeles,
Los Angeles, CA, USA

M. M. Glymour
Department of Society, Human Development, and Health,
Harvard School of Public Health,
Boston, MA, USA

E. Mormino
Department of Neurology, Harvard Medical School,
Boston, MA, USA

S. Mukherjee · P. K. Crane
Department of Medicine, University of Washington,
Seattle, WA, USA

C. DeCarli
Department of Neurology and Center for Neuroscience,
University of California at Davis,
Sacramento, CA, USA

deficits in AD and MCI. For memory, hypometabolism in similar regions of the parietal and temporal lobes were significantly associated with reduced performance in the MCI group. However, for the AD group, memory performance was significantly associated with metabolism in frontal and orbitofrontal areas, suggesting the possibility of compensatory metabolic activity in these areas. Overall, the associations between brain metabolism and cognition in this study suggest the importance of parietal and temporal lobar regions in memory and executive function in the early stages of disease and an increased importance of frontal regions for memory with increasing impairment.

Keywords Mild cognitive impairment (MCI) · Alzheimer's disease (AD) · FDG PET · Memory · Executive function

Introduction

Metabolic brain deficits as a consequence of early Alzheimer's disease measured using [^{18}F]fluorodeoxyglucose positron emission tomography (FDG PET) have been well established in the last two decades, with parietotemporal hypoactivity in AD patients the most consistent finding (Del Sole et al. 2008; Edison et al. 2007; Messa et al. 1994; Mielke et al. 1994; Piert et al. 1996). In addition, patients diagnosed with mild cognitive impairment (MCI), which is considered to be a prodromal stage of AD (Albert et al. 2011; Petersen 2000; Petersen et al. 1999), also show consistent brain metabolic reductions relative to healthy older adults (HC), particularly in regions of the parietal and temporal lobes (Del Sole et al. 2008; Li et al. 2008; Lowe et al. 2009; Mosconi et al. 2005). In addition to evaluating brain metabolism in MCI and AD for the purpose of understanding the impact of disease on resting-brain metabolism, FDG PET measures have also been assessed for sensitivity in early diagnosis, alone or in conjunction with other imaging modalities (e.g., magnetic resonance imaging (MRI)) and cerebrospinal fluid (CSF) protein levels (Chetelat et al. 2003b; de Leon et al. 2007; Drzezga et al. 2005; Habeck et al. 2008; Herholz et al. 2002; Kim et al. 2010; Lucignani and Nobili 2010; Minoshima et al. 1995; Mosconi 2005; Mosconi et al. 2010; Mosconi et al. 2004; Mosconi et al. 2007; Nobili et al. 2008; Pontecorvo and Mintun 2011; Rimajova et al. 2008; Silverman et al. 2001; von Borczyskowski et al. 2006). In addition, FDG PET scans have shown utility as part of a clinical diagnostic evaluation protocol and potentially in therapeutic intervention trials (Alexander et al. 2002; Bohnen et al. 2012; Chow et al. 2011; Herholz 1995; Jagust et al. 2007; Kono et al. 2007; Morinaga et al. 2010; Mosconi 2005; Noble and Scarmeas 2009; Poljansky et al. 2011; Reiman 2011). Overall, FDG PET measures have shown sensitivity to detecting brain metabolic decreases associated with AD, even in prodromal

stages, as well as utility for differential clinical diagnosis of AD (Herholz 2003).

The neuropsychological profile of Alzheimer's disease has been well-established with episodic memory and executive function deficits appearing early in the disease (Baudic et al. 2006; Stopford et al. 2010). Brain metabolic correlates of episodic memory in AD and MCI patients have been sought in a number of studies (Chetelat et al. 2003a; Desgranges et al. 1998; Desgranges et al. 2002; Edison et al. 2007; Eustache et al. 2001; Nishi et al. 2010; Perani et al. 1993; Schonknecht et al. 2011; Schonknecht et al. 2009; Slansky et al. 1995; Teipel et al. 2006). People with MCI and AD show significant associations between memory performance and FDG uptake in bilateral medial and lateral temporal, medial and lateral parietal, and frontal lobe regions. Executive function has been less investigated in relation to FDG PET measures in AD. A few studies have demonstrated significant associations between executive function and metabolism in the bilateral frontal, parietal, cingulate, and temporal cortices in patients with MCI and AD (Bracco et al. 2007; Collette et al. 1997; Collette et al. 2002; Kalpouzos et al. 2005; Kessler et al. 2000; Lee et al. 2008; Nestor et al. 1991; Nishi et al. 2010; Yun et al. 2011).

The Alzheimer's Disease Neuroimaging Initiative (ADNI) is a collaborative research effort that follows a cohort of more than 800 AD, MCI and HC participants longitudinally, with an extensive protocol of structural and molecular imaging, neuropsychological, and blood- and CSF-based evaluations (Mueller et al. 2005a; Mueller et al. 2005b; Weiner et al. 2010). This sample, which features repeated resting FDG PET scans and concurrent neuropsychological data in a sub-sample of participants, offers us an exciting opportunity to investigate the metabolic correlates of memory and executive function. To date, a number of studies have assessed the sensitivity of FDG PET scans as biomarkers for AD in the ADNI cohort. The majority of these studies have focused on differences in resting brain metabolism between diagnostic groups and the utility of FDG PET measures in predicting future clinical decline. In the ADNI cohort, patients with MCI and AD at baseline show reduced metabolism in the bilateral medial and lateral parietal lobe, medial and lateral temporal lobe, and frontal lobe (Haense et al. 2009; Jagust et al. 2010; Jagust et al. 2009; Karow et al. 2010; Landau et al. 2010; Langbaum et al. 2009). Patients with MCI and AD also show faster rates of longitudinal metabolic decline in frontal, parietal, and temporal lobes than HC participants (Chen et al. 2010; Lo et al. 2011). Measures of brain metabolism at baseline also predict future clinical conversion from MCI to probable AD in this sample, both alone and in combination with other biomarkers (i.e., MRI, CSF, cognition) (Chen et al. 2011; Herholz et al. 2011; Jagust et al. 2010; Landau et al. 2010; Walhovd et al. 2010a). Baseline and longitudinal change in FDG PET measures of brain metabolism are also associated with baseline and clinical dementia severity and baseline and

longitudinal change in general cognition measured using the Mini-Mental State Exam (MMSE) and/or the Alzheimer's Disease Assessment Schedule—Cognition subscale (ADAS-Cog) (Haense et al. 2009; Herholz et al. 2011; Jagust et al. 2010; Jagust et al. 2009; Landau et al. 2011; Landau et al. 2010; Langbaum et al. 2009; Lo et al. 2011; Walhovd et al. 2010a). Baseline measures of medial temporal lobe metabolism were associated with memory across the full sample, and separately among groups consisting of people with MCI and people with AD (Walhovd et al. 2010b). In addition, a measure of the extent to which a participant expresses an AD-like pattern of hypometabolism, the hypometabolic convergence index (HCI), was shown to be associated with memory, executive function, fluency and naming, as well as other cognitive performance across the full sample (Chen et al. 2011).

To date, no studies have evaluated the relationship between FDG PET measures of brain metabolism and cognition on a voxel-wise basis and within only AD and MCI participants. Therefore, the goal of the present study was to assess the brain metabolic correlates of executive function and memory in patients with AD and MCI. We chose to assess the relationship between brain metabolism and cognition on a whole brain voxel-wise basis with no a priori assumptions about the anatomical regions included in the analysis. Further, psychometrically optimized composite scores of memory and executive function (as described in companion articles in this Special Issue) have been used as the independent variables for our analyses, affording us additional confidence about the robustness of our findings. Finally, brain-cognition correlations were pursued within each diagnostic group (HC, MCI, and AD) separately to exclude potential confounding effects of disease severity. We hypothesized that brain metabolism in the bilateral parietal and frontal lobes would be associated with executive function, while metabolism in the bilateral parietal and temporal lobes would be associated with memory in patients with MCI and AD.

Methods

Alzheimer's Disease Neuroimaging Initiative (ADNI)

All individuals whose data were used in the preparation of this article were participants of the ADNI project (http://adni.loni.ucla.edu/). ADNI was launched in 2003 to evaluate biomarkers of AD-related neuropathology in patients with mild cognitive impairment (MCI) and early AD. This multi-site longitudinal study is supported by the National Institute on Aging (NIA), the National Institute of Biomedical Imaging and Bioengineering (NIBIB), the Food and Drug Administration (FDA), private pharmaceutical companies and non-profit organizations. The ADNI participants were recruited from 59 sites across the U.S. and Canada and include approximately 200 cognitively normal older individuals (healthy controls (HC)), 400 patients diagnosed with MCI, and 200 patients diagnosed with early probable AD aged 55–90 years. Written informed consent was obtained from all participants and the study was conducted with prior Institutional Review Board approval at each participating institution. Inclusion and exclusion criteria, clinical and neuroimaging protocols, and other information about ADNI has been published previously and can be found at www.adni-info.org. All demographic information, neuropsychological test scores, and diagnostic information were downloaded from the ADNI clinical data repository (http://www.loni.ucla.edu/ADNI/). Three hundred and fifty seven participants (86 AD, 185 MCI and 86 HC at baseline) in the ADNI cohort with initial PET scans were included in the present analyses (Table 1). The ADNI data contain a detailed neuropsychological assessment including measures of memory and executive function. Composite scores for memory and executive function were calculated by applying modern psychometric theory to item-level data from the ADNI neuropsychological battery (see explanation below, and the companion papers in this issue for details (Crane et al. 2011 submitted; Gibbons et al. 2011 submitted).

Neural data and sample characteristics

We evaluated data for 357 participants, of whom 86 had a diagnosis of AD, 185 had a diagnosis of MCI, and 86 were healthy controls (HC) at baseline. Demographic characteristics, including age, sex and years of education, were compared between diagnostic groups using a one-way analysis of variance (ANOVA) model and the results are summarized in Table 1.

Years of education differed significantly across groups; however, the main brain-cognition analyses presented in this report were conducted within each diagnostic group, obviating concerns of across-group comparisons. Further, age, sex, and years of education were used as nuisance covariates even for these within-group analyses.

Table 1 Sample demographic information

	AD (n=86)	MCI (n=185)	HC (n=86)
Age (mean±std)	75.8±7.4	75.4±7.1	76.0±4.8
Sex	53 M, 33 F	128 M, 58 F	53 M, 33 F
Years Education (mean±std) *	14.8±3.0	15.8±2.9	15.8±2.9
CDR Sum of Boxes (mean±std) *	4.51±1.59	1.55±0.80	0.04±0.14

Composite scores for memory and executive function

Detailed methods for the development of psychometrically sophisticated scores for memory (Crane et al. 2011 submitted) and executive functioning (Gibbons et al. 2011 submitted) for the ADNI data set ("ADNI-Mem" and "ADNI-Exec", respectively) are reported elsewhere in this issue. Briefly, item-level data from the ADNI neuropsychological battery were evaluated using confirmatory factor analysis approaches. A bi-factor model was used to generate executive functioning scores, while a single factor model was used for memory scores. Validation studies suggested excellent performance of these composite scores in a variety of analyses, as detailed in the other publications in this special issue. We used ADNI-Exec and ADNI-Mem in all analyses reported here.

Spatial normalization and reference scaling of FDG PET images

We downloaded FDG-PET data from the ADNI-LONI (http://adni.loni.ucla.edu/ADNI) in their most processed form (i.e., with the string 'Coreg,_Avg,_Std_Img_and_Vox_Siz,_Uniform_Resolution' in their filenames), as previously described (Jagust et al. 2010). Briefly, these scans were converted from their raw format to a single 30–60 min mean image, normalized to standard AC-PC space, intensity normalized using a subject-specific mask so that the global mean of all voxels in the mask is 1, and smoothed to generate a final image with 8 mm FWHM. The group-level analysis required further spatial and intensity normalization. First, all downloaded scans were spatially normalized by coregistration to a MNI space-aligned template using SPM8 (http://www.fil.ion.ucl.ac.uk/spm/software/spm8). We then scaled each image on a subject-by-subject basis using the mean intensity value extracted from a cerebellar reference region using a $3 \times 3 \times 3$ voxel cube centered on MNI=[0, −55, −32] within the cerebellar vermis.

Evaluation of the effects of diagnosis on brain metabolism

For validation purposes, we ran an overall diagnostic comparison in which we combined all 357 FDG-PET scans into a single regression model with diagnostic group (coded as 1/2/3 for HC/MCI/AD) as the independent variable. We evaluated the following regression model of a linear association with disease stage:

$$y = [\textbf{DXNUM}, \textbf{AGE}, \textbf{YEDU}, \textbf{SEX}, \textbf{1}]^* \beta + \varepsilon$$

where y denotes the FDG-PET signal at each voxel across all participants, **DXNUM** represents diagnostic group, **AGE**, **YEDU**, and **SEX** denote age, years of education,

and sex, 1 represents the intercept term, β is a 5 x 1 vector of regression weights, and ε is the residual unexplained by the model. Of the regression weights in β we are only interested in the first component, since age, years of education, and sex are nuisance covariates that appear in the model as silent regressors (i.e., they account for unwanted variance in the signal which is otherwise of no interest). Results were masked using a whole brain mask to exclude non-brain regions from the analysis and thresholded at $p<0.001$ (FWE correction for multiple comparisons) and a minimum cluster size (cs) of 50 voxels.

Brain-cognition association analyses

We performed all analyses in parallel in SPM8 using a multiple linear regression model within each of the three baseline diagnostic groups (HC, MCI, AD). The regression models can be written as:

$$Y = [\textbf{INDEP}, \textbf{AGE}, \textbf{YEDU}, \textbf{SEX}, \textbf{CDR} - \textbf{SB}, \textbf{1}]^* \beta + \varepsilon$$

where y denotes the FDG-PET signal at each voxel across all participants, **AGE**, **YEDU**, and **SEX** denote age, years of education, and sex, **1** represents the intercept term, β is a 6×1 vector of regression weights, and ε is the residual unexplained by the model. Additionally, we also included a covariate of disease severity within diagnostic category: the Clinical Dementia Rating scale "Sum of Boxes" score (**CDR-SB**). This score displays significant colinearity of an expected negative sign with ADNI-Mem in people with AD ($R=-0.25$, $p=0.02$) and MCI ($R=-0.14$, $p=0.05$), and with ADNI-Exec in people with MCI ($R=-0.22$, $p=0.002$) and healthy controls ($R=-0.21$, $p=0.05$). Thus, in order to establish the metabolic substrates of cognitive phenotypes above and beyond dementia severity even within diagnostic category, we included CDR-SB as an additional nuisance covariate in all 6 voxel-wise analyses. Of course, despite this attempt, we must concede that disease severity probably is a multidimensional entity, and there might still be differences in it that are not captured by CDR-SB; thus we cannot fully conclude that our findings have been disentangled from disease severity.

All results were again masked using a whole brain mask. For the analysis of ADNI-Exec in AD participants only and ADNI-Mem in both AD and MCI participants, results were displayed at a significance threshold of $p<0.001$ (uncorrected for multiple comparisons) and minimum cluster size (cs) of 50 contiguous voxels. If the results are displayed in SPM5, all analyses meet the $p<0.05$ (FDR correction for multiple comparisons) statistical threshold. However this option is not available in SPM8, therefore, we chose to use the

p<0.001 (uncorrected) threshold. For the ADNI-Exec analysis in MCI participants, the p<0.001 (uncorrected) threshold resulted in significant voxels across nearly the entire brain. Since we were interested in regional topography of brain-behavior associations, we chose to display this analysis (ADNI-Exec in MCI participants only) at a more stringent threshold of p<0.05 (FWE correction for multiple comparisons) and a cs of 50 voxels. All voxel-wise and cluster-wise statistical results are indicated in Tables 2, 3, 4, 5, and 6.

Finally, we used the client version of Talairach Daemon (http://www.talairach.org/index.html) (Lancaster et al. 1997) for anatomical localization of super-threshold maxima from all analyses. Specifically, we list nearest gray-matter locations within a maximum of 1 cm for the identified local maxima in Tables 2, 3, 4, 5, and 6.

Permutation test of group differences for voxel-wise association between metabolism and composite scores

We anticipate stronger brain-cognition relationships with increasing disease severity, and wanted to perform a

rigorous statistical comparison of AD and MCI groups in terms of brain-cognition associations with ADNI-Mem and ADNI-Exec. Such a comparison would require a complex general linear model for diagnostic status and its interaction with the composite scores. To avoid such a model, we decided to perform a simpler permutation test instead. The permutation test starts with the general linear models for both AD and MCI groups, but now arbitrarily swaps people from the AD group into the MCI group, and vice versa, keeping the overall group strengths intact. We performed 1,000 such permutations; each time running voxel-wise regressions and retaining voxel beta weights for the correlation between brain signal and outcome measure. For each permutation we thus obtain a difference in beta weights at each voxel

$$\Delta\beta(\text{voxel}) = \beta_{\text{AD}}(\text{voxel}) - \beta_{\text{MCI}}(\text{voxel})$$

The empirically generated null-distribution of $\Delta\beta$ for each voxel is then used to determine the p-value for the observed point estimate of $\Delta\beta$, i.e. the value obtained with the intact group assignment. The test proceeded in a two-

Table 2 Metabolic correlates of diagnostic group

FWE p	T-value	unc p	MNI-X	MNI-Y	MNI-Z	Lobe	Nearest Gyrus/Structure	Brodmann Area
<0.001	7.99	<0.001	6	−52	28	Right Limbic Lobe	Cingulate Gyrus	BA 31
<0.001	7.75	<0.001	−44	−72	38	Left Parietal Lobe	Inferior Parietal Lobule	BA 39
<0.001	7.69	<0.001	−6	−56	28	Left Limbic Lobe	Cingulate Gyrus	BA 31
<0.001	7.55	<0.001	14	−66	32	Right Parietal Lobe	Precuneus	BA 7
<0.001	7.51	<0.001	−50	−68	32	Left Parietal Lobe	Angular Gyrus	BA 39
<0.001	7.49	<0.001	−4	−70	34	Left Parietal Lobe	Precuneus	BA 7
<0.001	7.29	<0.001	−38	−62	42	Left Parietal Lobe	Inferior Parietal Lobule	BA 7
<0.001	7.22	<0.001	−32	−32	−12	Left Temporal Lobe	Hippocampus	n/a
<0.001	7.2	<0.001	−18	2	−34	Left Limbic Lobe	Uncus	BA 36
<0.001	7.14	<0.001	−48	−62	42	Left Parietal Lobe	Inferior Parietal Lobule	BA 40
<0.001	7.1	<0.001	−34	−20	−20	Left Limbic Lobe	Parahippocampal Gyrus, Hippocampus	n/a
<0.001	7.01	<0.001	−64	−38	−16	Left Temporal Lobe	Middle Temporal Gyrus	BA 21
<0.001	6.92	<0.001	−62	−42	−18	Left Temporal Lobe	Middle Temporal Gyrus	BA 20
<0.001	6.78	<0.001	−60	−50	−16	Left Temporal Lobe	Middle Temporal Gyrus	BA 37
<0.001	6.62	<0.001	−66	−26	−14	Left Temporal Lobe	Middle Temporal Gyrus	BA 21
<0.001	6.54	<0.001	−62	−18	−26	Left Temporal Lobe	Inferior Temporal Gyrus	BA 20
<0.001	6.13	<0.001	−26	−12	−36	Left Limbic Lobe	Uncus	BA 28
<0.001	5.82	<0.001	−42	−58	8	Left Temporal Lobe	Middle Temporal Gyrus	BA 39
0.001	5.68	<0.001	−6	−12	10	Left Subcortical	Thalamus, Medial Dorsal Nucleus	n/a
0.001	5.65	<0.001	−42	−46	−8	Left Limbic Lobe	Parahippocampal Gyrus	BA 19
0.001	5.61	<0.001	−42	−54	−2	Left Temporal Lobe	Sub-Gyral White Matter	n/a
<0.001	7.55	<0.001	48	−62	44	Right Parietal Lobe	Inferior Parietal Lobule	BA 40
<0.001	7.27	<0.001	64	−34	−20	Right Temporal Lobe	Inferior Temporal Gyrus	BA 20

MNI coordinates and labels of regions that decrease in relative metabolic activity with increasing disease severity, at a family-wise corrected p-threshold of p<0.05 and and a cluster-size threshold (cs)=50 voxels. There were no regions that increased in relative metabolic activity with increasing disease severity. The results for this regression model are only shown in this table (i.e., no graphical figure appears in the manuscript).

Table 3 Regions with a significant association between metabolism and executive function in AD

FWE p	T-value	unc p	MNI-X	MNI-Y	MNI-Z	Lobe	Nearest Gyrus/Structure	Brodmann Area
0.099	4.87	<0.001	−42	−74	38	Left Parietal Lobe	Precuneus	BA 19
0.267	4.53	<0.001	−38	−64	42	Left Parietal Lobe	Inferior Parietal Lobule	BA 39
0.488	4.28	<0.001	−52	−76	−16	Left Cerebellum	Declive	n/a
0.172	4.69	<0.001	4	−52	−44	Right Cerebellum	Cerebellar Tonsil	n/a
0.238	4.57	<0.001	56	−72	−16	Right Cerebellum	Declive	n/a
0.341	4.43	<0.001	−26	−6	48	Left Frontal Lobe	Middle Frontal Gyrus	BA 6
0.533	4.23	<0.001	−38	6	60	Left Frontal Lobe	Middle Frontal Gyrus	BA 6
0.857	3.09	<0.001	−48	8	48	Left Frontal Lobe	Middle Frontal Gyrus	BA 6
0.662	4.11	<0.001	40	−70	30	Right Temporal Lobe	Middle Temporal Gyrus	BA 39
0.882	3.87	<0.001	24	−62	22	Right Occipital Lobe	Precuneus	BA 31
0.971	3.67	<0.001	32	−68	22	Right Occipital Lobe	Superior Occipital Gyrus	BA 39
0.698	4.08	<0.001	−12	18	40	Left Limbic Lobe	Cingulate Gyrus	BA 32
0.931	3.78	<0.001	−28	18	40	Left Frontal Lobe	Middle Frontal Gyrus	BA 8
0.938	3.77	<0.001	−8	−78	50	Left Parietal Lobe	Precuneus	BA 7

MNI coordinates and labels of regions with a positive association between the brain metabolism and executive function (ADNI-Exec) people with AD, at an uncorrected p-threshold of p<0.001 and cs=50 voxels. There were no regions with a negative correlation.

tailed manner and identified significant AD/MCI differences in the brain-cognition correlations in both directions.

Results

Sample demographic and psychometric characteristics

Significant differences were observed between diagnostic groups in years of education (Table 1; $F_{2,354}$=3.55, p=0.03), and between baseline ADNI-Mem and ADNI-Exec scores (Fig. 1), as would be expected.

Effects of diagnostic group on brain metabolism

Diagnostic group was significantly associated with brain metabolism, controlling for the confounding influences of age, sex and education. Specifically, the present analysis reproduced the typical bilateral parietotemporal pattern of AD-related hypometabolism, with progressive reduction in brain metabolism associated with increasing disease severity (Table 2). No regions with AD-related hypermetabolism (i.e., increased metabolism associated with increasing disease severity) were observed.

Table 4 Regions with a significant association between metabolism and executive function in MCI

FWE p	T-value	unc p	MNI-X	MNI-Y	MNI-Z	Lobe	Nearest Gyrus/Structure	Brodmann Area
<0.001	6.3	<0.001	−46	−76	38	Left Parietal Lobe	Angular Gyrus	BA 39
<0.001	5.99	<0.001	−52	−56	28	Left Parietal Lobe	Supramarginal Gyrus	BA 40
<0.001	5.97	<0.001	−30	−72	38	Left Parietal Lobe	Precuneus	BA 19
0.001	5.82	<0.001	46	−58	0	Right Temporal Lobe	Middle Temporal Gyrus	BA 37
0.013	5.21	<0.001	56	−58	−16	RightTemporal Lobe	Middle Temporal Gyrus	BA 37
0.001	5.77	<0.001	−46	2	−8	Left Temporal Lobe	Superior Temporal Gyrus	BA 22
0.028	5.01	<0.001	−42	8	−20	Left Temporal Lobe	Superior Temporal Gyrus	BA 38
0.003	5.56	<0.001	50	−48	48	Right Parietal Lobe	Inferior Parietal Lobule	BA 40
0.003	5.53	<0.001	46	−54	52	Right Parietal Lobe	Inferior Parietal Lobule	BA 40
0.005	5.44	<0.001	60	−48	40	Right Parietal Lobe	Inferior Parietal Lobule	BA 40
0.003	5.55	<0.001	−54	−60	−18	Left Temporal Lobe	Inferior Temporal Gyrus	BA 20
0.011	5.25	<0.001	−52	−40	−18	Left Temporal Lobe	Middle Temporal Gyrus	BA 20
0.024	5.05	<0.001	−60	−34	−20	Left Temporal Lobe	Inferior Temporal Gyrus	BA 20
0.012	5.23	<0.001	62	−44	4	Right Temporal Lobe	Middle Temporal Gyrus	BA 22

MNI coordinates and labels of regions with a positive association between FDG PET measures of brain metabolism and executive function (ADNI-Exec) in MCI participants, at family-wise corrected p-threshold of p<0.05 and cs=50 voxels. There were no regions with a negative correlation.

Table 5 Regions with a significant association between metabolism and memory in AD

FWE p	T-value	unc p	MNI-X	MNI-Y	MNI-Z	Lobe	Nearest Gyrus/Structure	Brodmann Area
0.4253	4.3399	<0.001	−44	54	−10	Left Frontal Lobe	Middle Frontal Gyrus	Brodmann area 11
0.437	4.3277	<0.001	−52	−2	−36	Left Temporal Lobe	Inferior Temporal Gyrus	Brodmann area 20
0.4486	4.3158	<0.001	−42	10	−24	Left Temporal Lobe	Superior Temporal Gyrus	Brodmann area 38
0.4724	4.2919	<0.001	−6	14	−22	Left Frontal Lobe	Rectal Gyrus	Brodmann area 11
0.5508	4.216	<0.001	14	72	−4	Right Frontal Lobe	Superior Frontal Gyrus	Brodmann area 10
0.6287	4.1426	<0.001	6	−52	−44	Right Posterior Lobe	Cerebellar Tonsil	n/a
0.7447	4.03	<0.001	36	44	−18	Right Frontal Lobe	Middle Frontal Gyrus	Brodmann area 11
0.8493	3.9123	<0.001	30	28	−26	Right Frontal Lobe	Inferior Frontal Gyrus	Brodmann area 11
0.9599	3.7129	<0.001	−26	20	40	Left Frontal Lobe	Middle Frontal Gyrus	Brodmann area 8
0.9705	3.6776	<0.001	−16	50	42	Left Frontal Lobe	Superior Frontal Gyrus	Brodmann area 8

MNI coordinates and labels of regions with a positive association between the brain metabolism and memory (ADNI-Mem) in people with AD, at an uncorrected p-threshold of p<0.001 and cs=50 voxels. There were no regions with a negative correlation.

Table 6 Regions with a significant association between metabolism and memory in MCI

FWE p	T-value	unc p	MNI-X	MNI-Y	MNI-Z	Lobe	Nearest Gyrus/Structure	Brodmann Area
0.0484	4.8637	<0.001	−4	−72	36	Left Parietal Lobe	Precuneus	Brodmann area 7
0.0674	4.7747	<0.001	2	−38	36	Right Limbic Lobe	Cingulate Gyrus	Brodmann area 31
0.0699	4.7647	<0.001	−4	−76	48	Left Parietal Lobe	Precuneus	Brodmann area 7
0.1086	4.6414	<0.001	−30	−42	−6	Left Temporal Lobe	Sub-Gyral	Hippocampus
0.8542	3.7969	<0.001	−34	−34	−14	Left Limbic Lobe	Parahippocampal Gyrus	Brodmann area 36
0.999	3.3295	<0.001	−12	−32	8	Left Sub-lobar	Thalamus	Pulvinar
0.1777	4.4949	<0.001	−54	−46	54	Left Parietal Lobe	Inferior Parietal Lobule	Brodmann area 40
0.8359	3.8181	<0.001	−42	−58	50	Left Parietal Lobe	Inferior Parietal Lobule	Brodmann area 40
0.851	3.8007	<0.001	−32	−56	42	Left Parietal Lobe	Inferior Parietal Lobule	Brodmann area 40
0.537	4.0925	<0.001	50	−52	54	Right Parietal Lobe	Inferior Parietal Lobule	Brodmann area 40
0.9999	3.1949	<0.001	46	−64	48	Right Parietal Lobe	Inferior Parietal Lobule	Brodmann area 40
0.7185	3.9349	<0.001	−58	−34	−22	Left Temporal Lobe	Inferior Temporal Gyrus	Brodmann area 20
0.9984	3.3596	<0.001	−68	−26	−14	Left Temporal Lobe	Middle Temporal Gyrus	Brodmann area 21
0.7682	3.8884	<0.001	−32	14	−48	Left Temporal Lobe	Superior Temporal Gyrus	Brodmann area 38
0.9947	3.4379	<0.001	−42	−4	−50	Left Temporal Lobe	Inferior Temporal Gyrus	Brodmann area 20
0.8068	3.8497	<0.001	−2	18	72	Left Frontal Lobe	Superior Frontal Gyrus	Brodmann area 6
0.8859	3.7562	<0.001	28	−8	−26	Right Limbic Lobe	Parahippocampal Gyrus	Hippocampus
0.9654	3.6027	<0.001	20	0	−28	Right Limbic Lobe	Uncus	Brodmann area 28
0.9965	3.4092	<0.001	34	−18	−20	Right Limbic Lobe	Parahippocampal Gyrus	Hippocampus
0.8892	3.7516	<0.001	−26	42	14	Left Limbic Lobe	Anterior Cingulate	Brodmann area 32
0.9424	3.6612	<0.001	−26	32	24	Left Frontal Lobe	Medial Frontal Gyrus	Brodmann area 9
0.9158	3.7111	<0.001	−24	−18	−34	Left Limbic Lobe	Parahippocampal Gyrus	Brodmann area 35
0.9946	3.4398	<0.001	−20	−28	−30	Left Cerebellum	Culmen	n/a
0.999	3.3302	<0.001	−28	−14	−26	Left Limbic Lobe	Parahippocampal Gyrus	Hippocampus
0.923	3.6988	<0.001	28	−34	12	Right Sub-lobar	Caudate	Caudate Tail
0.9334	3.6796	<0.001	4	−8	10	Right Sub-lobar	Thalamus	n/a
0.9824	3.536	<0.001	0	34	32	Midline Limbic Lobe	Cingulate Gyrus	Brodmann area 32
0.9896	3.4909	<0.001	−2	24	42	Left Frontal Lobe	Cingulate Gyrus	Brodmann area 32

MNI coordinates and labels of regions with a positive association between brain metabolism and memory (ADNI-Mem) in people with MC, at an uncorrected p-threshold of p<0.001 and cs=50 voxels. There were no regions with a negative correlation.
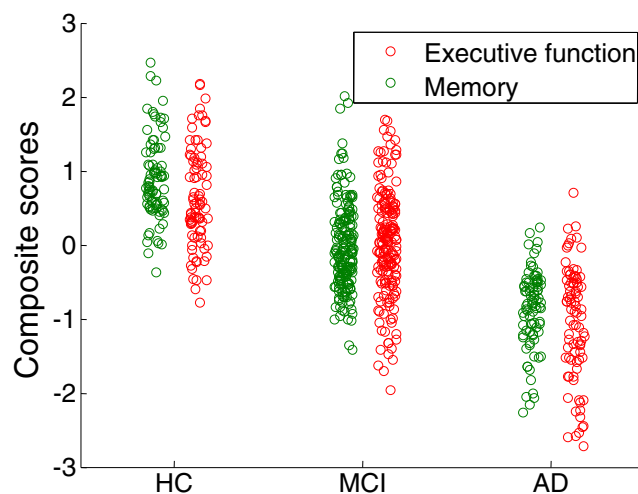
Fig. 1 Memory and Executive Function Composite Scores by Diagnostic Group. Scatter plots of memory and executive function composite scores across diagnostic groups. The ADNI-Exec score is plotted in red, the ADNI-Mem score is plotted in green. Both show strong associations with diagnosis (AD, MCI, HC)

Brain correlates of executive functioning and memory in AD, MCI, and HC

Topographic results for areas showing a significant positive association between brain metabolism and executive function in AD and MCI are shown in Fig. 2. In addition, a detailed listing of the anatomical location of supra-threshold clusters can be found in Tables 3, and 4. The most notable observed feature of these findings is that the ADNI-Exec was positively associated with brain metabolism in a mainly bilateral network consisting of occipital, temporal and parietal regions, but not frontal regions in AD and MCI participants. The most significant associations are in the left parietal lobe in AD and in bilateral parietal lobes in MCI. In addition, substantial overlap of associations in the AD and the MCI groups is demonstrated in the left lateral and medial parietal lobe (magenta color, Fig. 2). No significant associations between brain metabolism and executive functioning were observed in HC.

For the relationship between FDG PET and memory performance, AD and MCI groups showed markedly different topographic profiles of significant associations. In AD participants, increased metabolism in orbitofrontal and frontal lobar regions was significantly associated with better memory performance (higher ADNI-Mem; Fig. 3 and Table 5). However, MCI participants show very little frontal involvement (apart from pre SMA in BA 6; Fig. 3 and Table 6). Instead, significant positive associations between brain metabolism and memory performance were primarily observed in posterior areas, including in the parietal and temporal lobes with the largest cluster in the precuneus and posterior cingulate gyrus. Similar to ADNI-Exec, no significant associations between brain metabolism and memory factor were observed in the HC group.
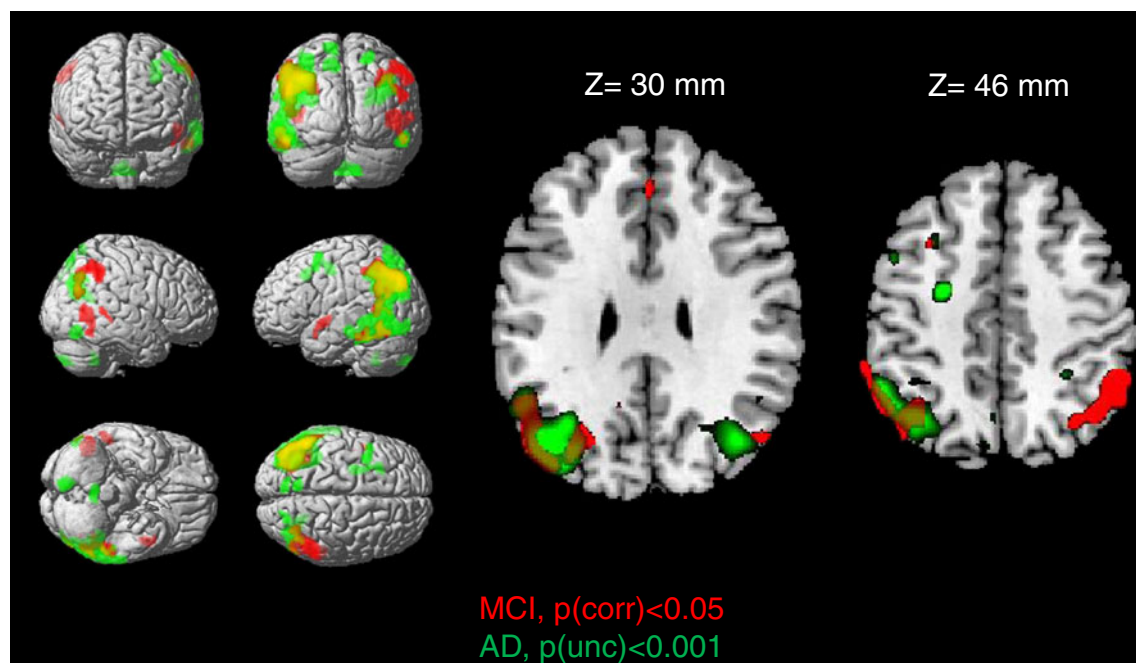

Fig. 2 Relationship between brain metabolism and executive function in patients with MCI and AD. Visualization of super-threshold local maxima in rendered surface images and selected axial slices for the topography of associations between FDG PET measures of brain metabolism and executive function (ADNI-Exec), displayed for both AD (*green*; p<0.001, uncorrected for multiple comparisons, minimum cluster size (cs)=50 voxels) and MCI (*red*; p<0.05, FWE correction for multiple comparisons, cs= 50 voxels). Significant associations in both groups were primarily observed in bilateral parietal and temporal lobes. In addition, notable overlap of regions with significant associations are observed (*yellow*)
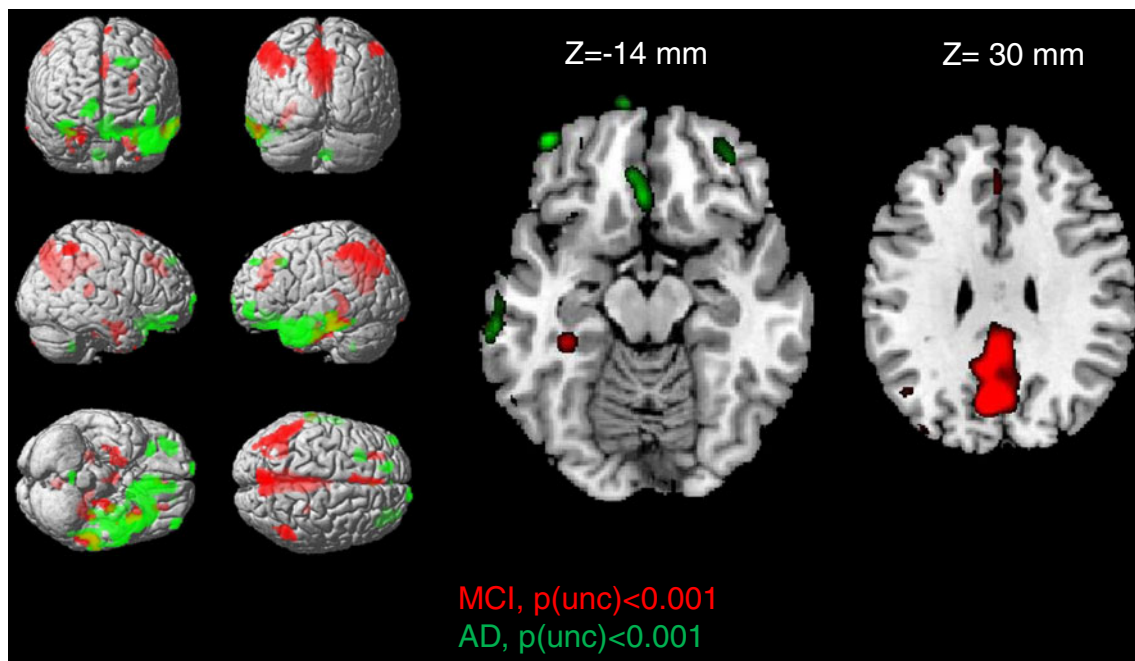
Fig. 3 Relationship between brain metabolism and memory in MCI and AD. Visualization of super-threshold local maxima in rendered surface images and selected axial slices for the topography of associations between brain metabolism and memory (ADNI-Mem) are displayed for both AD (green; p<0.001 (unc), cs=50 voxels) and MCI (*red*; p<0.001 (unc), cs=50 voxels). Significant associations were observed in the frontal lobes in the AD participants and the bilateral parietal and temporal lobes in the MCI participants. In contrast to the ADNI-Exec-score, there is minimal overlap of anatomical distribution in the AD and MCI associations and a noticeable anterior-posterior difference. These results suggest that the metabolic correlates of memory change the course of disease, shifting from a posterior parietotemporal pattern to a more frontal distribution

Overall, no negative associations between brain metabolism and either cognitive measure (ADNI-Exec or ADNI-Mem) were found at the p<0.001 (uncorrected) statistical threshold in any of the diagnostic groups.

Slope differences between MCI and AD as ascertained by the permutation test

Results of the permutation tests showed slope differences in the brain-cognition relationships, albeit at a reduced level of significance (Fig. 4 and Table 7). We found that few voxels reached p(unc)<0.001, so we dropped the threshold to p<0.01. Despite the marginal significance, one can visually appreciate the similarities and consistencies with the results from Figs. 2 and 3: for ADNI-Exec—people with MCI show a larger slope in the brain-cognition relationships in posterior areas, while people with AD show a large slope in mid-frontal areas. For ADNI-Mem people with AD show a larger brain behavioral slope in ventral frontal areas.

However, we stress that the results did not reach a level of significance of p<0.001, let alone a level that survives a family-wise error correction. The results thus only hint at possible differences that could be recovered if subject numbers were boosted substantially.

Discussion

In the present report, we identified a subset of regions in the AD-related parietotemporal hypometabolic pattern that are associated with impairment in executive function in MCI and AD patients, as well as memory in MCI patients. Interestingly, the metabolic correlates of memory among AD patients was quite different and involved primarily frontal and orbitofrontal areas, possibly suggesting at a shift from the disease-affected parietotemporal areas to more frontal areas. No significant associations were observed in HC participants between brain metabolism and cognition.

Brain-cognition associations in MCI and AD patients

The observed associations between executive function and brain metabolism in the medial and lateral parietal and temporal lobes in patients with MCI and AD is similar to results found in previous studies in smaller samples (Bracco et al. 2007; Collette et al. 1997; Kalpouzos et al. 2005; Lee et al. 2008; Nishi et al. 2010; Yun et al. 2011). Furthermore, the observed associations of memory with frontal brain metabolism in patients with AD and parietal and temporal metabolism in MCI are also similar to previous reports (Chetelat et al. 2003a; Desgranges et al. 1998; Desgranges
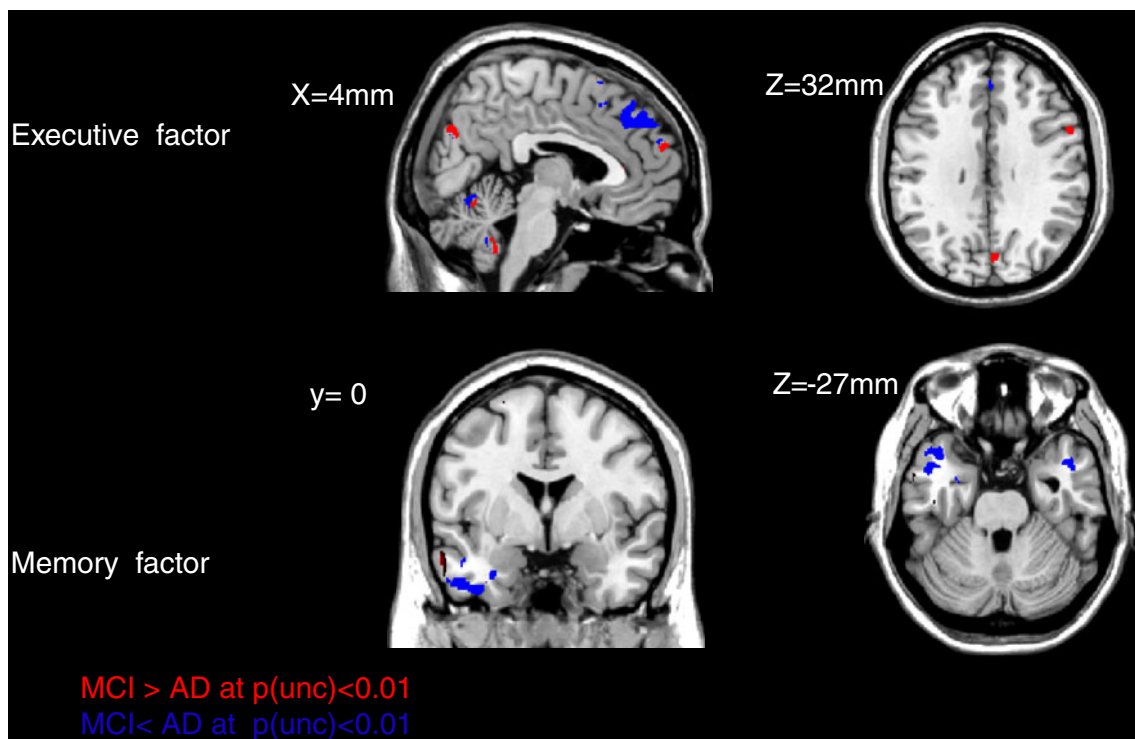
Fig. 4 Relationship between brain metabolism and memory in MCI and AD. Visualization of super-threshold local maxima in selected coronal, sagittal and axial slices for the areas that show significant difference between people with AD and MCI in the slope of the association between metabolism and cognitive outcome measures (executive function: top row, memory: bottom row). Areas where MCIs display a larger slope than ADs are marked in red, areas where ADs display a larger slope than MCIs are marked in blue. The p-level was obtained from a permutation test with 1,000 iterations and thresholded at p(unc)<0.01

et al. 2002; Edison et al. 2007; Eustache et al. 2001; Nishi et al. 2010; Perani et al. 1993; Schonknecht et al. 2011; Schonknecht et al. 2009; Slansky et al. 1995; Teipel et al. 2006). These associations suggest a functional network of frontal, temporal and parietal regions that are involved in memory and executive function. Extensive atrophy and reductions in neuronal function in MCI and AD in these regions may be responsible for the declines in memory and executive function observed in these patients.

Frontal metabolic activity associated with better memory performance among people with AD: re-allocation or selective disruption?

The metabolic association profiles of executive function in both MCI and AD, as well as the profile of memory in MCI, are located within widespread parieto-temporal cluster that has been demonstrated to show disease-related hypometabolism in numerous previous reports. On the other hand, the association profile of memory in AD patients is dramatically different and exclusively involves frontal and orbitofrontal regions. This observation may suggest a neuronal re-allocation of memory-related metabolic activity from the posterior cortex to the frontal cortex in AD *in response to increasing disease severity*. Since we did not consider repeated evaluations of the same individuals in the present analysis, disease severity was only an across-subjects factor and the potential observed re-allocation is only a cross-sectional phenomenon. To establish a true re-allocation independent confirmation in longitudinal data are obviously needed.

Compensatory re-allocation implies a shift of memory processing from posterior to anterior areas *within subject*; for a memory decrease from time 1 to time 2 this dictates a *positive* correlation with the metabolic signal in the area that is the origin point of the shift and a *negative* correlation with the metabolic signal in the destination point of the shift. An alternative model would be a selective disruption of memory-processing neural circuits with worsening disease severity: in a disease-free stage the implementation of memory processing might be redundant and involve a multitude of circuits that are employed in a subject-specific manner. As observed in our results, across people this heterogeneity in the profile of circuit utilization might preclude the emergence of focal areas of significance when testing the brain-cognition relationship. After the onset of symptoms with MCI, selected circuits might gradually be more disrupted and affected, uncovering brain-cognition relationships that were hidden because of super-imposed variability before.

These two conceptual models, re-allocation vs. selective disruption, cannot be disentangled in a relative sense: every re-allocation is a selective disruption if the absolute magnitude of metabolic signals cannot be discerned. Absolute quantification of metabolic signals will thus be necessary to distinguish between the two scenarios: in contrast to selective disruption, compensatory re-allocation would imply an *absolute* increase in the metabolic signal in the areas to which the re-allocation occurs. A consequence that both models have in common is a change in the rank order of cognitive performance for an ideal cohort of disease patients who start from similar disease stages and undergo disease changes at a similar pace. Patients who started with *worse* performance might end up in a better position relative to their peers, if the latter are affected with more disruption or less ability for successful re-allocation.

Longitudinal follow-up and data from the study arms ADNI GO and ADNI2 present an exciting test bed for these ideas in the near future.

Lack of findings in healthy controls

No significant associations between resting brain metabolism and cognition were observed in HC in the present study. As can be discerned from Fig. 1, within-group variability of both ADNI-Mem and ADNI-Exec is comparable across the three diagnostic groups, so the lack of a brain-cognition correlation cannot be attributed to a restricted range of the behavioral scores in the healthy controls.

We can thus ask further whether the controls fail to exhibit sufficient *neural* variability to manifest a correlation and whether adding more observations would likely increase the statistical power, based on the sub-threshold observed for the healthy controls. We performed 2 supplementary analyses to address these questions.

(1)   We took the voxel location that showed the most reliable correlation between metabolism and ADNI-Mem (p(unc)=0.0019, MNI=[24, −92, −10], Fusiform gyrus, BA 18). We generated Gaussian-distributed values of all independent variables and residuals based on observed sample means and variances, and took the regression weights from the point estimate for this particular voxel location for 1,000 iterations, varying the numbers of people (from 10 to 500 in increments of 10). For the data that were constructed in these simulations, we then generated a power curve and plotted the fraction of iterations that gave a significant correlation with ADNI-Mem as a function of sample size (graph not shown). A power of 0.8 was obtained for 270 people. (Adding additional observations from the new diagnostic category "Early MCI" from study extensions ADNI GO and ADNI 2 might present an opportunity to substantiate this extrapolation).

(2)   We checked all 89 voxel locations reported in Tables 2, 3, 4, 5, and 6, and computed the ratio of metabolic sample variances of the healthy control participants versus the combined pool of MCI and AD participants. We performed a permutation version of an F-test for the equality of variance with 10,000 iterations for each location. None of the 89 locations yielded significant differences between healthy controls and the MCI/AD participants, confirming the impression from visual inspection that variability is well matched across diagnostic groups.

The results of these additional analyses argue against notable brain-cognition correlations that are obscured because of a lack of variability. However, substantially boosting sample sizes by a factor 3 or more might achieve sufficient power to detect brain-cognition correlations in the healthy controls. (In this light, the significant brain-cognition relationships in the AD group, which had equal numeric strength as the HC group, are even more impressive.)

Unique contributions and limitations

This study provides a unique contribution to the current literature by assessing the relationship between brain metabolism and cognition in the largest sample of AD, MCI, and HC participants evaluated to date. Further, we used psychometrically sophisticated composite measures of memory and executive function that combine the results from multiple assessments, which may provide a better estimate of actual cognitive status than the results from a single test. Finally, the use of voxel-wise analysis techniques allow analysis of brain metabolism across the entire brain without any a priori assumptions, which may allow for identification of potentially novel regions associated with memory and executive function. The fact that parieto-temporal regions were identified in this analysis provides further evidence regarding the importance of metabolic reductions in these regions as mediators of AD-related cognitive dysfunction. Furthermore, the relatively novel identification of the association of hypometabolism in frontal regions with memory dysfunction in AD may not have been identified with region of interest or whole brain metabolic pattern techniques.

Despite the significant contributions of the present study, a few limitations are notable. First, this analysis used only cross-sectional FDG PET and psychometric data. Therefore, the assessment of brain-behavior relationships was limited to between-subject comparisons. Any conclusions drawn about changes in metabolism in relation to increasing disease severity and cognitive decline were preliminary, as other factors could explain between-subject differences in

Table 7 Regions that show a significant difference between people with MCI and AD in the association of metabolism and memory/executive function

MNI-X	MNI-Y	MNI-Z	p(unc)	Sign	Lobe	Structure/Gyrus	Brodmann Area
EF							
2	62	20	0.001	MCI>AD	Right Frontal Lobe	Medial Frontal Gyrus	Brodmann area 10
2	−52	−38	0.001		Right Cerebellum	Nodule	n/a
6	−62	−12	0.001		Right Cerebellum	Culmen	n/a
4	−76	32	0.003		Right Occipital Lobe	Cuneus	Brodmann area 7
54	12	34	0.005		Right Frontal Lobe	Middle Frontal Gyrus	Brodmann area 9
2	−54	−38	0.001	MCI<AD	Right Cerebellum	Nodule	n/a
4	50	42	0.001		Right Frontal Lobe	Medial Frontal Gyrus	Brodmann area 9
4	42	48	0.001		Right Frontal Lobe	Medial Frontal Gyrus	Brodmann area 8
−50	4	−8	0.001		Left Temporal Lobe	Superior Temporal Gyrus	Brodmann area 22
6	−62	−10	0.002		Right Cerebellum	Culmen	n/a
2	40	30	0.005		Right Frontal Lobe	Medial Frontal Gyrus	Brodmann area 9
MEM							
−2	−52	−42	0.001	MCI>AD	Left Cerebellum	Cerebellar Tonsil	n/a
−60	0	−20	0.002		Left Temporal Lobe	Middle Temporal Gyrus	Brodmann area 21
−42	54	−10	0.002		Left Frontal Lobe	Middle Frontal Gyrus	Brodmann area 11
−56	4	−30	0.003		Left Temporal Lobe	Middle Temporal Gyrus	Brodmann area 21
−50	12	−34	0.003		Left Temporal Lobe	Middle Temporal Gyrus	Brodmann area 21
6	−8	12	0.003		Right Sub-lobar	Thalamus	n/a
14	−14	14	0.003		Right Sub-lobar	Thalamus	n/a
−12	12	−22	0.004		Left Frontal Lobe	Medial Frontal Gyrus	Brodmann area 25
−44	−14	−30	0.005		Left Temporal Lobe	Fusiform Gyrus	Brodmann area 20
−10	−84	38	0.005	MCI<AD	Parietal Lobe	Precuneus	Brodmann area 19
−42	−8	−34	0.001		Left Temporal Lobe	Inferior Temporal Gyrus	Brodmann area 20
−2	−54	−38	0.001		Left Cerebellum	Nodule	n/a
32	30	0	0.001		Right Frontal Lobe	Inferior Frontal Gyrus	Brodmann area 47
−46	16	−34	0.001		Left Temporal Lobe	Superior Temporal Gyrus	Brodmann area 38
−56	4	−32	0.002		Left Temporal Lobe	Middle Temporal Gyrus	Brodmann area 21
−46	2	−24	0.002		Left Temporal Lobe	Middle Temporal Gyrus	Brodmann area 21
−40	−10	18	0.002		Left Sub-lobar	Insula	Brodmann area 13
0	28	−16	0.002		Midline Frontal Lobe	Medial Frontal Gyrus	Brodmann area 25
6	−52	−46	0.002		Right Cerebellum	Cerebellar Tonsil	n/a
44	10	−26	0.002		Right Temporal Lobe	Superior Temporal Gyrus	Brodmann area 38
−2	−74	10	0.003		Left Occipital Lobe	Cuneus	Brodmann area 18
36	50	−16	0.003		Right Frontal Lobe	Superior Frontal Gyrus	Brodmann area 11
−46	12	−22	0.004		Right Temporal Lobe	Superior Temporal Gyrus	Brodmann area 38
−36	30	2	0.004		Left Frontal Lobe	Inferior Frontal Gyrus	Brodmann area 47
−8	16	−22	0.004		Left Frontal Lobe	Rectal Gyrus	Brodmann area 11
−30	0	−30	0.005		Left Limbic Lobe	Uncus	Amygdala
36	4	14	0.005		Right Sub-lobar	Insula	Brodmann area 13
−38	8	−30	0.008		Left Temporal Lobe	Superior Temporal Gyrus	Brodmann area 38

MNI coordinates and labels of regions with a group difference between AD and MCI in the association between brain metabolism and memory/executive function and at an uncorrected p-threshold of $p<0.01$ and cs=10 voxels. The results were obtained from a permutation test with 1,000 iterations. The smallest recordable p-level is thus 0.001. "MCI>AD" indicates that the slope of the association was larger in the MCI group, while "MCI<AD" denotes the converse scenario.

metabolism and/or cognition. Future studies utilizing longitudinal FDG PET and neuropsychological test data will help

to elucidate relationships between changes in brain metabolism and progressive decline in memory and executive

function within subjects. The present study also limited the disease-related differences in metabolism to a simple multiple regression model that does not address the possible unique contributions of each disease stage. Further, quadratic or u-shaped associations with disease severity could not be assessed. For our discovery of brain-cognition relationships we performed linear regression within each diagnostic group separately. This is a compromise that offers analytical tractability, while allowing for disease-stage specific changes in the associations between cognition and brain metabolism. Future studies could evaluate more sophisticated and complex models that incorporate metabolic changes in a longitudinal framework. Ideally this would be performed in larger samples with sufficient power for estimation of non-linear and higher dimensional models. Finally, a number of other variables of interest, which may modulate the relationship of brain metabolism and cognition, were not included in the presented analyses. For example, genetic variation may be an important factor mediating brain-cognition relationships. In fact, a previous study demonstrated a significant effect of apolipoprotein E (APOE) genotype on brain metabolism in the ADNI cohort (Langbaum et al. 2009). Therefore, future studies could evaluate the role of APOE and other genetic variants in modulating relationships between brain metabolism and memory and executive function. Future studies could also exploit the multi-modal nature of ADNI and use information about brain structure as an additional covariate (Kanda et al. 2008; Samuraki et al. 2007). The goal of such a study would be to identify metabolic correlates of disease severity, memory and executive function *above and beyond* the effects explained by atrophy and cortical thinning, which can be expected to occur in the course of the disease. Such 'metabolic density' profiles or, in other words, topographic patterns of metabolic activity per conserved unit of gray matter, might yield valuable knowledge about AD-related neural changes and/or provide additional diagnostic and predictive information for disease identification and monitoring. Other variables have also been shown to affect brain metabolism and/or cognition, including the presence of amyloid deposition (Li et al. 2008; Mormino et al. 2009) and cerebrovascular changes (Brickman et al. 2011; Carmichael et al. 2010). Future studies could evaluate the role of other independent variables in mediating the relationship between brain metabolism and cognition.

Summary and conclusions

In conclusion, we observed significant positive associations between brain metabolism measured using FDG PET and executive function and memory in patients with MCI and AD, but not in HC. Impairments in executive function were associated with parietotemporal hypometabolism in both MCI and AD. On the other hand, impaired memory was associated with reduced metabolism in parietotemporal regions in MCI patients and frontal regions in AD patients. Overall, the results of the present study underscore the importance of changes in brain metabolism in the cognitive impairment seen in the prodromal and early stages of AD.

References

Albert, M. S., DeKosky, S. T., Dickson, D., Dubois, B., Feldman, H. H., Fox, N. C., & Phelps, C. H. (2011). The diagnosis of mild cognitive impairment due to Alzheimer's disease: Recommendations from the National Institute on Aging-Alzheimer's Association workgroups on diagnostic guidelines for Alzheimer's disease. *Alzheimer's & Dementia, 7*(3), 270–279. doi:10.1016/j.jalz.2011.03.008.

Alexander, G. E., Chen, K., Pietrini, P., Rapoport, S. I., & Reiman, E. M. (2002). Longitudinal PET evaluation of cerebral metabolic decline in dementia: A potential outcome measure in Alzheimer's disease treatment studies. *The American Journal of Psychiatry, 159*(5), 738–745.

Baudic, S., Barba, G. D., Thibaudet, M. C., Smagghe, A., Remy, P., & Traykov, L. (2006). Executive function deficits in early Alzheimer's disease and their relations with episodic memory. *Archives of Clinical Neuropsychology, 21*(1), 15–21. doi:10.1016/j.acn.2005.07.002.

Bohnen, N. I., Djang, D. S., Herholz, K., Anzai, Y., & Minoshima, S. (2012). Effectiveness and safety of 18F-FDG PET in the evaluation of dementia: A review of the recent literature. *Journal of Nuclear Medicine, 53*(1), 59–71. doi:10.2967/jnumed.111.096578.

Bracco, L., Bessi, V., Piccini, C., Mosconi, L., Pupi, A., & Sorbi, S. (2007). Metabolic correlates of executive dysfunction. Different

patterns in mild and very mild Alzheimer's disease. *Journal of Neurology, 254*(8), 1052–1065. doi:10.1007/s00415-006-0488-1.

Brickman, A. M., Siedlecki, K. L., Muraskin, J., Manly, J. J., Luchsinger, J. A., Yeung, L. K., & Stern, Y. (2011). White matter hyperintensities and cognition: Testing the reserve hypothesis. *Neurobiology of Aging, 32*(9), 1588–1598. doi:10.1016/j.neurobiolaging.2009.10.013.

Carmichael, O., Schwarz, C., Drucker, D., Fletcher, E., Harvey, D., Beckett, L., & DeCarli, C. (2010). Longitudinal changes in white matter disease and cognition in the first year of the Alzheimer disease neuroimaging initiative. *Archives of Neurology, 67*(11), 1370–1378. doi:10.1001/archneurol.2010.284.

Chen, K., Ayutyanont, N., Langbaum, J. B., Fleisher, A. S., Reschke, C., Lee, W., & Reiman, E. M. (2011). Characterizing Alzheimer's disease using a hypometabolic convergence index. *NeuroImage, 56*(1), 52–60. doi:10.1016/j.neuroimage.2011.01.049.

Chen, K., Langbaum, J. B., Fleisher, A. S., Ayutyanont, N., Reschke, C., Lee, W., & Reiman, E. M. (2010). Twelve-month metabolic declines in probable Alzheimer's disease and amnestic mild cognitive impairment assessed using an empirically pre-defined statistical region-of-interest: Findings from the Alzheimer's Disease Neuroimaging Initiative. *NeuroImage, 51*(2), 654–664. doi:10.1016/j.neuroimage.2010.02.064.

Chetelat, G., Desgranges, B., de la Sayette, V., Viader, F., Berkouk, K., Landeau, B., & Eustache, F. (2003). Dissociating atrophy and hypometabolism impact on episodic memory in mild cognitive impairment. *Brain, 126*(Pt 9), 1955–1967. doi:10.1093/brain/awg196.

Chetelat, G., Desgranges, B., de la Sayette, V., Viader, F., Eustache, F., & Baron, J. C. (2003). Mild cognitive impairment: Can FDG-PET predict who is to rapidly convert to Alzheimer's disease? *Neurology, 60*(8), 1374–1377.

Chow, T. W., Graff-Guerrero, A., Verhoeff, N. P., Binns, M. A., Tang-Wai, D. F., Freedman, M., & Pollock, B. G. (2011). Open-label study of the short-term effects of memantine on FDG-PET in frontotemporal dementia. *Neuropsychiatric Disease and Treatment, 7*, 415–424. doi:10.2147/NDT.S22635.

Collette, F., Salmon, E., Van der Linden, M., Degueldre, C., & Franck, G. (1997). Functional anatomy of verbal and visuospatial span tasks in Alzheimer's disease. [Clinical Trial Controlled Clinical Trial Research Support, Non-U.S. Gov't]. *Human Brain Mapping, 5*(2), 110–118.

Collette, F., Van der Linden, M., Delrue, G., & Salmon, E. (2002). Frontal hypometabolism does not explain inhibitory dysfunction in Alzheimer disease. [Research Support, Non-U.S. Gov't]. *Alzheimer Disease and Associated Disorders, 16*(4), 228–238.

Crane, P. K., Carle, A., Gibbons, L. E., Insel, P., Mackin, R. S., Gross, A., . . . for the Alzheiemer's Disease Neuroimaging Initiative. (2011). Development and assessment of a composite score for memory in the Alzheimer's Disease Neuroimaging Initiative (ADNI). *Brain Imaging and Behavior.*

de Leon, M. J., Mosconi, K., Blennow, K., DeSanti, S., Zinkowski, R., Mehta, P. D., & Rusinek, H. (2007). Imaging and CSF studies in the preclinical diagnosis of Alzheimer's disease. *Annals of the New York Academy of Sciences, 1097*, 114–145. doi:10.1196/annals.1379.012.

Del Sole, A., Clerici, F., Chiti, A., Lecchi, M., Mariani, C., Maggiore, L., & Lucignani, G. (2008). Individual cerebral metabolic deficits in Alzheimer's disease and amnestic mild cognitive impairment: An FDG PET study. *European Journal of Nuclear Medicine and Molecular Imaging, 35*(7), 1357–1366. doi:10.1007/s00259-008-0773-6.

Desgranges, B., Baron, J. C., de la Sayette, V., Petit-Taboue, M. C., Benali, K., Landeau, B., & Eustache, F. (1998). The neural substrates of memory systems impairment in Alzheimer's disease. A PET study of resting brain glucose utilization. *Brain, 121*(Pt 4), 611–631.

Desgranges, B., Baron, J. C., Lalevee, C., Giffard, B., Viader, F., de La Sayette, V., & Eustache, F. (2002). The neural substrates of episodic memory impairment in Alzheimer's disease as revealed by FDG-PET: Relationship to degree of deterioration. *Brain, 125* (Pt 5), 1116–1124.

Drzezga, A., Grimmer, T., Riemenschneider, M., Lautenschlager, N., Siebner, H., Alexopoulus, P., & Kurz, A. (2005). Prediction of individual clinical outcome in MCI by means of genetic assessment and (18)F-FDG PET. *Journal of Nuclear Medicine, 46*(10), 1625–1632.

Edison, P., Archer, H. A., Hinz, R., Hammers, A., Pavese, N., Tai, Y. F., & Brooks, D. J. (2007). Amyloid, hypometabolism, and cognition in Alzheimer disease: An [11C]PIB and [18F]FDG PET study. *Neurology, 68*(7), 501–508. doi:10.1212/01.wnl.0000244749.20056.d4.

Eustache, F., Desgranges, B., Giffard, B., de la Sayette, V., & Baron, J. C. (2001). Entorhinal cortex disruption causes memory deficit in early Alzheimer's disease as shown by PET. *Neuroreport, 12*(4), 683–685.

Gibbons, L. E., Carle, A. C., Mackin, R. S., Harvey, D., Mukherjee, S., Insel, P., . . . for the Alzheiemer's Disease Neuroimaging Initiative. (2011). A composite score for executive functioning, validated in Alzheimer's Disease Neuroimaging Initiative (ADNI) participants with baseline mild cognitive impairment. *Brain Imaging and Behavior.*

Habeck, C., Foster, N. L., Perneczky, R., Kurz, A., Alexopoulos, P., Koeppe, R. A., & Stern, Y. (2008). Multivariate and univariate neuroimaging biomarkers of Alzheimer's disease. *NeuroImage, 40*(4), 1503–1515. doi:10.1016/j.neuroimage.2008.01.056.

Haense, C., Herholz, K., Jagust, W. J., & Heiss, W. D. (2009). Performance of FDG PET for detection of Alzheimer's disease in two independent multicentre samples (NEST-DD and ADNI). *Dementia and Geriatric Cognitive Disorders, 28*(3), 259–266. doi:10.1159/000241879.

Herholz, K. (1995). FDG PET and differential diagnosis of dementia. *Alzheimer Disease and Associated Disorders, 9*(1), 6–16.

Herholz, K. (2003). PET studies in dementia. *Annals of Nuclear Medicine, 17*(2), 79–89.

Herholz, K., Salmon, E., Perani, D., Baron, J. C., Holthoff, V., Frolich, L., & Heiss, W. D. (2002). Discrimination between Alzheimer dementia and controls by automated analysis of multicenter FDG PET. *NeuroImage, 17*(1), 302–316.

Herholz, K., Westwood, S., Haense, C., & Dunn, G. (2011). Evaluation of a calibrated (18)F-FDG PET score as a biomarker for progression in Alzheimer disease and mild cognitive impairment. *Journal of Nuclear Medicine, 52*(8), 1218–1226. doi:10.2967/jnumed.111.090902.

Jagust, W., Reed, B., Mungas, D., Ellis, W., & Decarli, C. (2007). What does fluorodeoxyglucose PET imaging add to a clinical diagnosis of dementia? *Neurology, 69*(9), 871–877. doi:10.1212/01.wnl.0000269790.05105.16.

Jagust, W. J., Bandy, D., Chen, K., Foster, N. L., Landau, S. M., Mathis, C. A., & Koeppe, R. A. (2010). The Alzheimer's Disease Neuroimaging Initiative positron emission tomography core. *Alzheimer's & Dementia, 6*(3), 221–229. doi:10.1016/j.jalz.2010.03.003.

Jagust, W. J., Landau, S. M., Shaw, L. M., Trojanowski, J. Q., Koeppe, R. A., Reiman, E. M., & Mathis, C. A. (2009). Relationships between biomarkers in aging and dementia. [Comparative Study Multicenter Study Research Support, N.I.H., Extramural Research Support, Non-U.S. Gov't Research Support, U.S. Gov't, Non-P.H.S.]. *Neurology, 73*(15), 1193–1199. doi:10.1212/WNL.0b013e3181bc010c.

Kalpouzos, G., Eustache, F., de la Sayette, V., Viader, F., Chetelat, G., & Desgranges, B. (2005). Working memory and FDG-PET dissociate early and late onset Alzheimer disease patients. *Journal of Neurology, 252*(5), 548–558. doi:10.1007/s00415-005-0685-3.

Kanda, T., Ishii, K., Uemura, T., Miyamoto, N., Yoshikawa, T., Kono, A. K., & Mori, E. (2008). Comparison of grey matter and metabolic reductions in frontotemporal dementia using FDG-PET and voxel-based morphometric MR studies. *European Journal of Nuclear Medicine and Molecular Imaging, 35*(12), 2227–2234. doi:10.1007/s00259-008-0871-5.

Karow, D. S., McEvoy, L. K., Fennema-Notestine, C., Hagler, D. J., Jr., Jennings, R. G., Brewer, J. B., & Dale, A. M. (2010). Relative capability of MR imaging and FDG PET to depict changes associated with prodromal and early Alzheimer disease. *Radiology, 256*(3), 932–942. doi:10.1148/radiol.10091402.

Kessler, J., Mielke, R., Grond, M., Herholz, K., & Heiss, W. D. (2000). Frontal lobe tasks do not reflect frontal lobe function in patients with probable Alzheimer's disease. *International Journal of Neuroscience, 104*(1–4), 1–15.

Kim, S. H., Seo, S. W., Yoon, D. S., Chin, J., Lee, B. H., Cheong, H. K., & Na, D. L. (2010). Comparison of neuropsychological and FDG-PET findings between early-versus late-onset mild cognitive impairment: A five-year longitudinal study. *Dementia and Geriatric Cognitive Disorders, 29*(3), 213–223. doi:10.1159/000278422.

Kono, A. K., Ishii, K., Sofue, K., Miyamoto, N., Sakamoto, S., & Mori, E. (2007). Fully automatic differential diagnosis system for dementia with Lewy bodies and Alzheimer's disease using FDG-PET and 3D-SSP. *European Journal of Nuclear Medicine and Molecular Imaging, 34*(9), 1490–1497. doi:10.1007/s00259-007-0380-y.

Lancaster, J. L., Rainey, L. H., Summerlin, J. L., Freitas, C. S., Fox, P. T., Evans, A. C., & Mazziotta, J. C. (1997). Automated labeling of the human brain: A preliminary report on the development and evaluation of a forward-transform method. *Human Brain Mapping, 5*(4), 238–242. doi:10.1002/(SICI)1097-0193(1997)5:4<238::AID-HBM6>3.0.CO;2-4.

Landau, S. M., Harvey, D., Madison, C. M., Koeppe, R. A., Reiman, E. M., Foster, N. L., & Jagust, W. J. (2011). Associations between cognitive, functional, and FDG-PET measures of decline in AD and MCI. *Neurobiology of Aging, 32*(7), 1207–1218. doi:10.1016/j.neurobiolaging.2009.07.002.

Landau, S. M., Harvey, D., Madison, C. M., Reiman, E. M., Foster, N. L., Aisen, P. S., & Jagust, W. J. (2010). Comparing predictors of conversion and decline in mild cognitive impairment. [Comparative Study Research Support, N.I.H., Extramural Research Support, Non-U.S. Gov't Research Support, U.S. Gov't, Non-P.H.S.]. *Neurology, 75*(3), 230–238. doi:10.1212/WNL.0b013e3181e8e8b8.

Langbaum, J. B., Chen, K., Lee, W., Reschke, C., Bandy, D., Fleisher, A. S., & Reiman, E. M. (2009). Categorical and correlational analyses of baseline fluorodeoxyglucose positron emission tomography images from the Alzheimer's Disease Neuroimaging Initiative (ADNI). *NeuroImage, 45*(4), 1107–1116. doi:10.1016/j.neuroimage.2008.12.072.

Lee, D. Y., Seo, E. H., Choo, I. H., Kim, S. G., Lee, J. S., Lee, D. S., & Woo, J. I. (2008). Neural correlates of the clock drawing test performance in Alzheimer's disease: A FDG-PET study. *Dementia and Geriatric Cognitive Disorders, 26*(4), 306–313. doi:10.1159/000161055.

Li, Y., Rinne, J. O., Mosconi, L., Pirraglia, E., Rusinek, H., DeSanti, S., & de Leon, M. J. (2008). Regional analysis of FDG and PIB-PET images in normal aging, mild cognitive impairment, and Alzheimer's disease. *European Journal of Nuclear Medicine and Molecular Imaging, 35*(12), 2169–2181. doi:10.1007/s00259-008-0833-y.

Lo, R. Y., Hubbard, A. E., Shaw, L. M., Trojanowski, J. Q., Petersen, R. C., Aisen, P. S., & Jagust, W. J. (2011). Longitudinal change of biomarkers in cognitive decline. *Archives of Neurology, 68*(10), 1257–1266. doi:10.1001/archneurol.2011.123.

Lowe, V. J., Kemp, B. J., Jack, C. R., Jr., Senjem, M., Weigand, S., Shiung, M., & Petersen, R. C. (2009). Comparison of 18F-FDG and PiB PET in cognitive impairment. *Journal of Nuclear Medicine, 50*(6), 878–886. doi:10.2967/jnumed.108.058529.

Lucignani, G., & Nobili, F. (2010). FDG-PET for early assessment of Alzheimer's disease: Isn't the evidence base large enough? *European Journal of Nuclear Medicine and Molecular Imaging, 37*(8), 1604–1609. doi:10.1007/s00259-010-1535-9.

Messa, C., Perani, D., Lucignani, G., Zenorini, A., Zito, F., Rizzo, G., et al. (1994). High-resolution technetium-99 m-HMPAO SPECT in patients with probable Alzheimer's disease: Comparison with fluorine-18-FDG PET. *Journal of Nuclear Medicine, 35*(2), 210–216.

Mielke, R., Pietrzyk, U., Jacobs, A., Fink, G. R., Ichimiya, A., Kessler, J., & Heiss, W. D. (1994). HMPAO SPET and FDG PET in Alzheimer's disease and vascular dementia: Comparison of perfusion and metabolic pattern. *European Journal of Nuclear Medicine, 21*(10), 1052–1060.

Minoshima, S., Frey, K. A., Koeppe, R. A., Foster, N. L., & Kuhl, D. E. (1995). A diagnostic approach in Alzheimer's disease using three-dimensional stereotactic surface projections of fluorine-18-FDG PET. *Journal of Nuclear Medicine, 36*(7), 1238–1248.

Morinaga, A., Ono, K., Ikeda, T., Ikeda, Y., Shima, K., Noguchi-Shinohara, M., & Yamada, M. (2010). A comparison of the diagnostic sensitivity of MRI, CBF-SPECT, FDG-PET and cerebrospinal fluid biomarkers for detecting Alzheimer's disease in a memory clinic. *Dementia and Geriatric Cognitive Disorders, 30*(4), 285–292. doi:10.1159/000320265.

Mormino, E. C., Kluth, J. T., Madison, C. M., Rabinovici, G. D., Baker, S. L., Miller, B. L., & Jagust, W. J. (2009). Episodic memory loss is related to hippocampal-mediated beta-amyloid deposition in elderly subjects. [Comparative Study Research Support, N.I.H., Extramural]. *Brain, 132*(5), 1310–1323. doi:10.1093/brain/awn320.

Mosconi, L. (2005). Brain glucose metabolism in the early and specific diagnosis of Alzheimer's disease. FDG-PET studies in MCI and AD. *European Journal of Nuclear Medicine and Molecular Imaging, 32*(4), 486–510. doi:10.1007/s00259-005-1762-7.

Mosconi, L., Berti, V., Glodzik, L., Pupi, A., De Santi, S., & de Leon, M. J. (2010). Pre-clinical detection of Alzheimer's disease using FDG-PET, with or without amyloid imaging. *Journal of Alzheimer's Disease, 20*(3), 843–854. doi:10.3233/JAD-2010-091504.

Mosconi, L., Perani, D., Sorbi, S., Herholz, K., Nacmias, B., Holthoff, V., & Pupi, A. (2004). MCI conversion to dementia and the APOE genotype: A prediction study with FDG-PET. *Neurology, 63*(12), 2332–2340.

Mosconi, L., Tsui, W. H., De Santi, S., Li, J., Rusinek, H., Convit, A., & de Leon, M. J. (2005). Reduced hippocampal metabolism in MCI and AD: Automated FDG-PET image analysis. *Neurology, 64*(11), 1860–1867. doi:10.1212/01.WNL.0000163856.13524.08.

Mosconi, L., Tsui, W. H., Pupi, A., De Santi, S., Drzezga, A., Minoshima, S., & de Leon, M. J. (2007). (18)F-FDG PET database of longitudinally confirmed healthy elderly individuals improves detection of mild cognitive impairment and Alzheimer's disease. *Journal of Nuclear Medicine, 48*(7), 1129–1134. doi:10.2967/jnumed.107.040675.

Mueller, S. G., Weiner, M. W., Thal, L. J., Petersen, R. C., Jack, C., Jagust, W., & Beckett, L. (2005a). The Alzheimer's disease neuroimaging initiative. *Neuroimaging Clinics of North America, 15*(4), 869–877. doi:10.1016/j.nic.2005.09.008. xi–xii.

Mueller, S. G., Weiner, M. W., Thal, L. J., Petersen, R. C., Jack, C. R., Jagust, W., & Beckett, L. (2005b). Ways toward an early diagnosis in Alzheimer's disease: The Alzheimer's Disease Neuroimaging Initiative (ADNI). *Alzheimer's & Dementia, 1*(1), 55–66. doi:10.1016/j.jalz.2005.06.003.

Nestor, P. G., Parasuraman, R., Haxby, J. V., & Grady, C. L. (1991). Divided attention and metabolic brain dysfunction in mild dementia of the Alzheimer's type. [Research Support, Non-U.S. Gov't Research Support, U.S. Gov't, P.H.S.]. *Neuropsychologia, 29*(5), 379–387.

Nishi, H., Sawamoto, N., Namiki, C., Yoshida, H., Dinh, H. D., Ishizu, K., & Fukuyama, H. (2010). Correlation between cognitive deficits and glucose hypometabolism in mild cognitive impairment. [Research Support, Non-U.S. Gov't]. *Journal of Neuroimaging, 20*(1), 29–36. doi:10.1111/j.1552-6569.2008.00328.x.

Nobili, F., Salmaso, D., Morbelli, S., Girtler, N., Piccardo, A., Brugnolo, A., & Pagani, M. (2008). Principal component analysis of FDG PET in amnestic MCI. *European Journal of Nuclear Medicine and Molecular Imaging, 35*(12), 2191–2202. doi:10.1007/s00259-008-0869-z.

Noble, J. M., & Scarmeas, N. (2009). Application of pet imaging to diagnosis of Alzheimer's disease and mild cognitive impairment. *International Review of Neurobiology, 84*, 133–149. doi:10.1016/S0074-7742(09)00407-3.

Perani, D., Bressi, S., Cappa, S. F., Vallar, G., Alberoni, M., Grassi, F., et al. (1993). Evidence of multiple memory systems in the human brain. A [18F]FDG PET metabolic study. *Brain, 116*(4), 903–919.

Petersen, R. C. (2000). Mild cognitive impairment: Transition between aging and Alzheimer's disease. *Neurologia, 15*(3), 93–101.

Petersen, R. C., Smith, G. E., Waring, S. C., Ivnik, R. J., Tangalos, E. G., & Kokmen, E. (1999). Mild cognitive impairment: Clinical characterization and outcome. *Archives of Neurology, 56*(3), 303–308.

Piert, M., Koeppe, R. A., Giordani, B., Berent, S., & Kuhl, D. E. (1996). Diminished glucose transport and phosphorylation in Alzheimer's disease determined by dynamic FDG-PET. *Journal of Nuclear Medicine, 37*(2), 201–208.

Poljansky, S., Ibach, B., Hirschberger, B., Manner, P., Klunemann, H., Hajak, G., & Marienhagen, J. (2011). A visual [18F]FDG-PET rating scale for the differential diagnosis of frontotemporal lobar degeneration. *European Archives of Psychiatry and Clinical Neuroscience, 261*(6), 433–446. doi:10.1007/s00406-010-0184-0.

Pontecorvo, M. J., & Mintun, M. A. (2011). PET amyloid imaging as a tool for early diagnosis and identifying patients at risk for progression to Alzheimer's disease. *Alzheimers Res Ther, 3*(2), 11. doi:10.1186/alzrt70.

Reiman, E. M. (2011). Fluorodeoxyglucose positron emission tomography: Emerging roles in the evaluation of putative Alzheimer's disease-modifying treatments. *Neurobiology of Aging, 32*(Suppl 1), S44–47. doi:10.1016/j.neurobiolaging.2011.09.007.

Rimajova, M., Lenzo, N. P., Wu, J. S., Bates, K. A., Campbell, A., Dhaliwal, S. S., & Martins, R. N. (2008). Fluoro-2-deoxy-D-glucose (FDG)-PET in APOEepsilon4 carriers in the Australian population. *Journal of Alzheimer's Disease, 13*(2), 137–146.

Samuraki, M., Matsunari, I., Chen, W. P., Yajima, K., Yanase, D., Fujikawa, A., & Yamada, M. (2007). Partial volume effect-corrected FDG PET and grey matter volume loss in patients with mild Alzheimer's disease. *European Journal of Nuclear Medicine and Molecular Imaging, 34*(10), 1658–1669. doi:10.1007/s00259-007-0454-x.

Schonknecht, O. D., Hunt, A., Toro, P., Guenther, T., Henze, M., Haberkorn, U., & Schroder, J. (2011). Bihemispheric cerebral FDG PET correlates of cognitive dysfunction as assessed by the CERAD in Alzheimer's disease. *Clinical EEG and Neuroscience, 42*(2), 71–76.

Schonknecht, O. D., Hunt, A., Toro, P., Henze, M., Haberkorn, U., & Schroder, J. (2009). Neural correlates of delayed episodic memory in patients with mild cognitive impairment–a FDG PET study. [Research Support, Non-U.S. Gov't]. *Neuroscience Letters, 467*(2), 100–104. doi:10.1016/j.neulet.2009.10.014.

Silverman, D. H., Small, G. W., Chang, C. Y., Lu, C. S., Kung De Aburto, M. A., Chen, W., & Phelps, M. E. (2001). Positron emission tomography in evaluation of dementia: Regional brain metabolism and long-term outcome. *Journal of the American Medical Association, 286*(17), 2120–2127.

Slansky, I., Herholz, K., Pietrzyk, U., Kessler, J., Grond, M., Mielke, R., & Heiss, W. D. (1995). Cognitive impairment in Alzheimer's disease correlates with ventricular width and atrophy-corrected cortical glucose metabolism. *Neuroradiology, 37*(4), 270–277.

Stopford, C. L., Thompson, J. C., Neary, D., Richardson, A. M., & Snowden, J. S. (2010). Working memory, attention, and executive function in Alzheimer's disease and frontotemporal dementia. *Cortex.* doi:10.1016/j.cortex.2010.12.002.

Teipel, S. J., Willoch, F., Ishii, K., Burger, K., Drzezga, A., Engel, R., & Hampel, H. (2006). Resting state glucose utilization and the CERAD cognitive battery in patients with Alzheimer's disease. *Neurobiology of Aging, 27*(5), 681–690. doi:10.1016/j.neurobiolaging.2005.03.015.

von Borczyskowski, D., Wilke, F., Martin, B., Brenner, W., Clausen, M., Mester, J., & Buchert, R. (2006). Evaluation of a new expert system for fully automated detection of the Alzheimer's dementia pattern in FDG PET. *Nuclear Medicine Communications, 27*(9), 739–743. doi:10.1097/01.mnm.0000230078.25609.2b.

Walhovd, K. B., Fjell, A. M., Brewer, J., McEvoy, L. K., Fennema-Notestine, C., Hagler, D. J., Jr., & Dale, A. M. (2010). Combining MR imaging, positron-emission tomography, and CSF biomarkers in the diagnosis and prognosis of Alzheimer disease. *AJNR. American Journal of Neuroradiology, 31*(2), 347–354. doi:10.3174/ajnr.A1809.

Walhovd, K. B., Fjell, A. M., Dale, A. M., McEvoy, L. K., Brewer, J., Karow, D. S., & Fennema-Notestine, C. (2010). Multi-modal imaging predicts memory performance in normal aging and cognitive decline. *Neurobiology of Aging, 31*(7), 1107–1121. doi:10.1016/j.neurobiolaging.2008.08.013.

Weiner, M. W., Aisen, P. S., Jack, C. R., Jr., Jagust, W. J., Trojanowski, J. Q., Shaw, L., & Schmidt, M. (2010). The Alzheimer's disease neuroimaging initiative: Progress report and future plans. *Alzheimer's & Dementia, 6*(3), 202–211. e207.

Yun, J. Y., Lee, D. Y., Seo, E. H., Choo, I. H., Park, S. Y., Kim, S. G., & Woo, J. I. (2011). Neural Correlates of Stroop Performance in Alzheimer's Disease: A FDG-PET Study. *Dement Geriatr Cogn Dis Extra, 1*(1), 190–201. doi:10.1159/000329517.